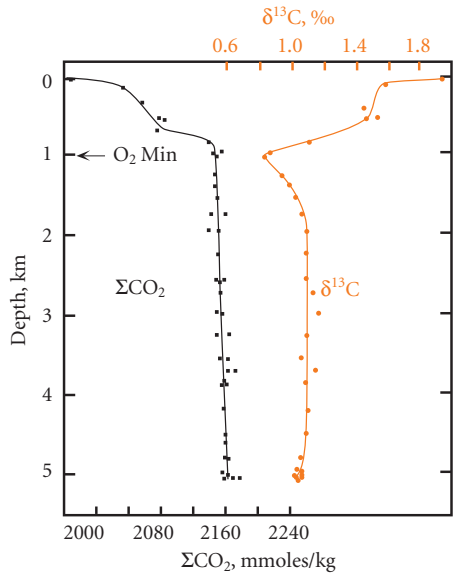

Figure 9.15 Depth profile of total dissolved inorganic carbon and $\delta^{13}C$ in the North Atlantic. Data from Kroopnick *et al.* (1972).

tions between dissolved inorganic carbon and organic carbon can be as low as 5‰ in algae.

Not surprisingly, the carbon isotope fractionation in C fixation is also temperature-dependent. Thus higher fractionations are observed in cold-water phytoplankton than in warm-water species. However, this observation also reflects a kinetic effect: there is generally less dissolved CO_2 available in warm waters because of the decreasing solubility with temperature. As a result, a larger fraction of the CO_2 is utilized and there is consequently less fractionation. Surface waters of the ocean are generally enriched in ^{13}C (relative to ^{12}C) because of uptake of ^{12}C during photosynthesis (Figure 9.15). The degree of enrichment depends upon the productivity: biologically productive areas show greater depletion. Deep water, on the other hand, is enriched in ^{12}C. Organic matter falls through the water column and is decomposed and "remineralized" (i.e., converted to inorganic carbon) by the action of bacteria, enriching deep water in ^{12}C and total DIC. Thus biological activity acts to "pump" carbon, and particularly ^{12}C from surface to deep waters.

Nearly all organic matter originates through photosynthesis. Subsequent reactions convert the photosynthetically produced carbohydrates to a variety of other organic compounds utilized by organisms. Further fractionations occur in these reactions. These fractionations are thought to be kinetic in origin and may partly arise from organic C-H bonds being enriched in ^{12}C and organic C-O bonds being enriched in ^{13}C. ^{12}C is preferentially consumed in respiration (again, because bonds are weaker and it reacts more rapidly), which enriches residual organic matter in ^{13}C. Thus the carbon isotopic composition of organisms becomes slightly more positive moving up the food chain.

The principal exception to the creation of organic matter through photosynthesis is *chemosynthesis*. In chemosynthesis, chemical reactions rather than light provide the energy to "fix" CO_2. Regardless of the energy source, however, fixation of CO_2 involves the Benson-Calvin Cycle and RUBISCO. Not surprisingly, then, chemosynthesis typically results in carbon isotope fractionations similar to those of photosynthesis. Thus large carbon isotope fractionations are the signature of both photosynthesis and chemosynthesis.

9.5.2 Nitrogen isotope fractionation in biological processes

Nitrogen is another important element in biological processes, being an essential component of all amino acids, proteins, and other key compounds such as RNA and DNA. There are five important forms of inorganic nitrogen: N_2, NO_3^-, NO_2^-, NH_3 and NH_4^+. Equilibrium isotope fractionations occur between these five forms, and kinetic fractionations occur during biological assimilation of nitrogen. Ammonia is the form of nitrogen that is ultimately incorporated into organic matter by growing plants. Most terrestrial plants depend on symbiotic bacteria for *fixation* (i.e., reduction) of N_2 and other forms of nitrogen to ammonia. Many plants, including many marine algae, can utilize oxidized nitrogen, $NO_3^-$and NO_2^-, and a few (blue-green algae and legumes, for example) are able to utilize N_2 directly. In these cases, nitrogen must first be reduced by the action of reductase enzymes. As with carbon, fractionation may occur in each of the several steps that occur in the nitrogen assimilation process. Denitrifying bacteria use nitrates as

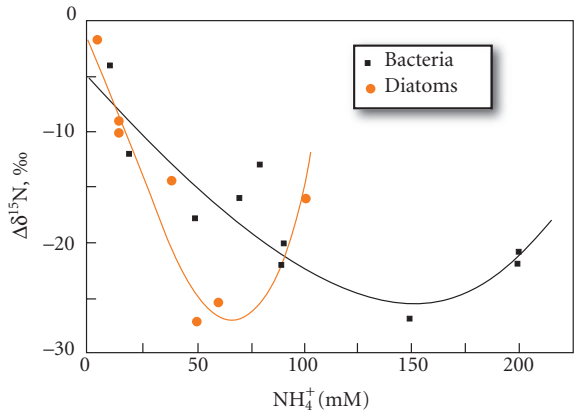

Figure 9.16 Dependence of nitrogen isotope fractionation by bacteria and diatoms on dissolved ammonium concentration. After Fogel and Cifuentes (1993). With kind permission of Springer Science+Business Media.

electron donors (i.e., as an oxidant) and reduce it without assimilating it. In this dissimilatory denitrification, there is a significant kinetic fractionation, with the light isotope, ^{14}N, being preferentially reduced leaving residual nitrate enriched in ^{15}N by 6–7‰.

While isotope fractionations during assimilation of ammonium are still poorly understood, it appears there is a strong dependence on the concentration of the ammonium ion. Such dependence has been observed, as for example in Figure 9.16. The complex dependence in Figure 9.16 is interpreted as follows. The increase in fractionation from highest to moderate concentrations of ammonium reflects the switching on of active ammonium transport by cells. At the lowest concentrations, essentially all available nitrogen is transported into the cell and assimilated, so there is little fractionation observed.

The isotopic compositions of marine particulate nitrogen and non-nitrogen-fixing plankton are typically −3‰ to +12‰ $\delta^{15}N$. Non-nitrogen fixing terrestrial plants unaffected by artificial fertilizers generally have a narrower range of +6‰ to +13 per mil. Marine blue-green algae range from −4 to +2, with most in the range of −4 to −2‰. Most nitrogen-fixing terrestrial plants fall in the range of −2 to +4‰, and hence are typically lighter than non-nitrogen fixing plants.

9.5.3 Oxygen and hydrogen isotope fractionation by plants

Oxygen is incorporated into biological material from CO_2, H_2O, and O_2. However, both CO_2 and O_2 are in oxygen isotopic equilibrium with water during photosynthesis, and water is the dominant source of O. Therefore, the isotopic composition of plant water determines the oxygen isotopic composition of plant material. The oxygen isotopic composition of plant material seems to be controlled by exchange reactions between water and carbonyl oxygens (oxygens doubly bound to carbon):

$$C{=}^{16}O + H_2^{18}O \rightarrow C{=}^{18}O + H_2^{16}O$$

Fractionations of +16 to +27‰ (i.e., the organically bound oxygen is heavier) have been measured for these reactions. Consistent with this, cellulose from most plants has $\delta^{18}O$ of +27 ± 3‰. Other factors, however, play a role in the oxygen isotopic composition of plant material. First, the isotopic composition of water varies from $\delta^{18}O \approx -55$‰ in Arctic regions to $\delta^{18}O \approx 0$‰ in the oceans. Second, less than complete equilibrium may be achieved if photosynthesis is occurring at a rapid pace, resulting in less fractionation. Finally, some fractionation of water may occur during transpiration, with residual water in the plant becoming heavier.

Hydrogen isotope fractionation during photosynthesis occurs such that the light isotope is enriched in organic material. In marine algae, isotope fractionations of −100 to −150‰ have been observed, which is a little more than that observed in terrestrial plants (−86 to −120‰). Among terrestrial plants, there appears to be a difference between C_3 and C_4 plants. The former show fractionations of −117 to −121‰, while fractionations of −86 to −109‰ have been observed in C_4 plants. However, little is known in detail about the exact mechanisms of fractionation.

As for oxygen, variations in the isotopic composition of available water and fractionation during transpiration are important in controlling the hydrogen isotopic composition of plants. This is illustrated in Figure 9.17.

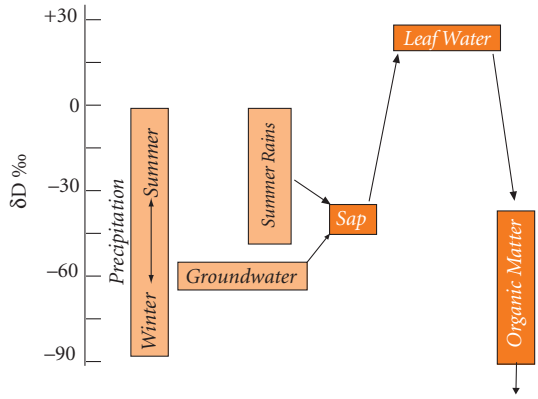

Figure 9.17 Isotopic fractionations of hydrogen during primary production in terrestrial plants. After Fogel and Cifuentes (1993). With kind permission of Springer Science+Business Media.

9.5.4 Biological fractionation of sulfur isotopes

Though essential to life, sulfur is a minor component in living tissue (C:S atomic ratio is about 200). Plants take up sulfur as sulfate and subsequently reduce it to sulfide and incorporate it into cysteine, an amino acid. There is apparently no fractionation of sulfur isotopes in transport across cell membranes and incorporation into cysteine, but there is a fractionation of +0.5 to −4.5‰ in the reduction process, referred to as *assimilatory sulfate reduction*. This is substantially less than the expected fractionation of about −20‰, suggesting that most sulfur taken up by primary producers is reduced and incorporated into tissue.

Sulfur, however, plays two other important roles in biological processes. First, sulfur, in the form of sulfate, can act as an electron acceptor or oxidant, and is utilized as such by sulfur-reducing bacteria. This process, in which H_2S is liberated, is called *dissimilatory sulfate reduction* and plays an important role in biogeochemical cycles, both as a sink for sulfur and a source for atmospheric oxygen. A large fractionation of +5 to −46‰ is associated with this process. This process produces by far the most significant fractionation of sulfur isotopes, and thus governs the isotopic composition of sulfur in the exogene. Sedimentary sulfate typically has $\delta^{34}S$ of about +17‰, which is similar to the isotopic composition of sulfate in the oceans (+20‰), while sedimentary sulfide has a $\delta^{34}S$ of around −18‰. The living biomass has a $\delta^{34}S$ of ≈0.

The final important role of sulfur is as a reductant. Sulfide is an electron acceptor used by some types of photosynthetic bacteria as well as other bacteria in the reduction of CO_2 to organic carbon. Unique among these perhaps are the chemosynthetic bacteria of submarine hydrothermal vents. They utilize H_2S emanating from the vents as an energy source and form the base of the food chain in these unique ecosystems. A fractionation of +2 to −18‰ is associated with this process.

9.5.5 Isotopes and diet: you are what you eat

As we have seen, the two main photosynthetic pathways, C_3 and C_4, lead to organic carbon with different carbon isotopic compositions. Terrestrial C_3 plants have $\delta^{13}C$ values that average about −27‰, C_4 plants an average $\delta^{13}C$ of about −13‰. Marine plants (which are all C_3) utilize dissolved bicarbonate rather than atmospheric CO_2. Seawater bicarbonate is about 8.5‰ heavier than atmospheric CO_2, and marine plants average about 7.5‰ heavier than terrestrial C_3 plants. In addition, because the source of the carbon they fix is isotopically more variable, the isotopic composition of marine plants is also more variable. Finally, marine cyanobacteria (blue-green algae) tend to fractionate carbon isotopes less during photosynthesis than do true marine plants, so they tend to average 2 to 3‰ higher in $\delta^{13}C$.

Plants may also be divided into two types based on their source of nitrogen: those that can utilize N_2 directly, and those that utilize only "fixed" nitrogen in ammonia and nitrate. The former include the legumes (e.g., beans, peas, etc.) and marine cyanobacteria. The legumes, which are exclusively C_3 plants, utilize both N_2 and fixed nitrogen, and have an average $\delta^{15}N$ of +1‰, whereas modern non-leguminous plants average about +3‰. Prehistoric non-leguminous plants were more positive, averaging perhaps +9‰, because the isotopic composition of present soil nitrogen has been affected by the use of chemical fertilizers. For both groups, there was probably a range in $\delta^{15}N$ of ±4 or 5‰, because the isotopic composition of soil nitrogen varies and there is some fractionation involved in uptake. Marine plants have $\delta^{15}N$ of +7 ± 5‰,

whereas marine cyanobacteria have $\delta^{15}N$ of $-1 \pm 3‰$. Thus, based on their $\delta^{13}C$ and $\delta^{15}N$ values, autotrophs can be divided into several groups, which are summarized in Figure 9.18.

DeNiro and Epstein (1978) studied the relationship between the carbon isotopic composition of animals and their diet. They found that there is only slight further fractionation of carbon by animals, and that the carbon isotopic composition of animal tissue closely reflects that of the animal's diet. Typically, carbon in animal tissue is about 1‰ heavier than their diet. The small fractionation between animal tissue and diet is a result of the slightly weaker bond formed by ^{12}C compared with ^{13}C. The weaker bonds are more readily broken during respiration, and, not surprisingly, the CO_2 respired by most animals investigated was slightly lighter than their diet. Thus only a small fractionation in carbon isotopes occurs as organic carbon passes up the food web. Terrestrial food chains usually do not have more than three trophic levels, implying a maximum further fractionation of +3‰; marine food chains can have up to seven trophic levels, implying a maximum carbon isotope difference between primary producers and top predators of 7‰. These differences are smaller than the range observed in primary producers.

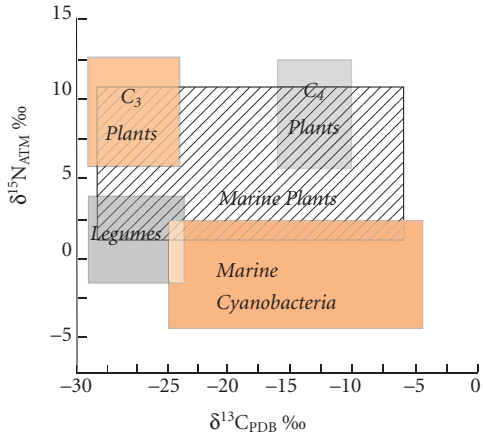

Figure 9.18 Relationship between $\delta^{13}C$ and $\delta^{15}N$ among the principal classes of autotrophs. Adapted from DeNiro (1987).

In another study, DeNiro and Epstein (1981) found that $\delta^{15}N$ of animal tissue reflects the $\delta^{15}N$ of the animal's diet, but is typically 3 to 4‰ higher than that of the diet. Thus in contrast to carbon, significant fractionation of nitrogen isotopes will occur as nitrogen passes up the food chain. These relationships are summarized in Figure 9.19. *The significance of these results is that it is possible to infer the diet of an animal from its carbon and nitrogen isotopic composition.*

Schoeninger and DeNiro (1984) found that the carbon and nitrogen isotopic composition of bone collagen in animals was similar to that of body tissue as a whole. Apatite in bone appears to undergo isotopic exchange with meteoric water once it is buried, but bone collagen and tooth enamel appear to be robust and retain their original isotopic compositions. This means that the nitrogen and carbon isotopic composition of fossil bone collagen

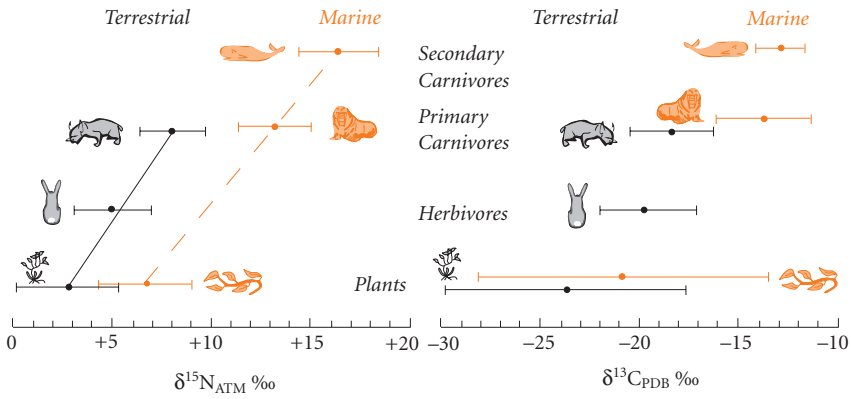

Figure 9.19 Values of $\delta^{13}C$ and $\delta^{15}N$ in various marine and terrestrial organisms. After Schoeninger and DeNiro (1984). With permission from Elsevier.

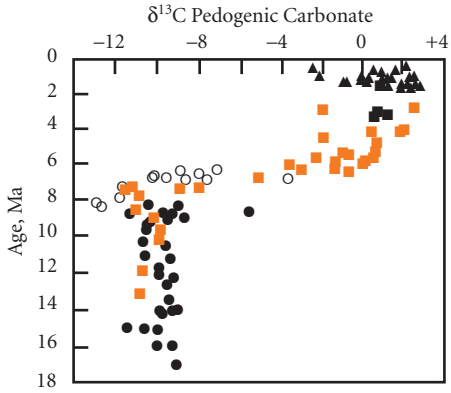

Figure 9.20 $\delta^{13}C$ in carbonates from paleosols of the Potwar Plateau in Pakistan. The change in $\delta^{13}C$ may reflect the evolution of C_4 plants. Reprinted by permission from McMillan Publishers Ltd: Quade *et al.* (1989).

and teeth can be used to reconstruct the diet of fossil animals.

Plant photosynthesis can also influence the isotopic composition of soil carbonate: when the plant dies, its organic carbon is incorporated into the soil and oxidized to CO_2 by bacteria and other soil organisms. In arid regions, some of this CO_2 precipitates as soil calcium carbonate. In an area of Pakistan presently dominated by C_4 grasses, Quade *et al.* (1989) found that a sharp shift in $\delta^{13}C$ in soil carbonate occurred about 7 million years ago (Figure 9.20). Quade *et al.* concluded that the shift marks the transition from C_3-dominant to C_4-dominant grasslands. They initially interpreted this as a response to the uplift of the Tibetan Plateau and the development of the monsoon. However, other evidence, including oxygen isotope data from Pakistani soil carbonates, suggests the monsoons developed about a million years earlier. Interestingly, other studies indicated that North American grasslands transitioned from dominance of C_3 to C_4 at about the same time. This synchronicity suggests a global cause, while the monsoons are a regional phenomenon. C_4 photosynthesis is more efficient at lower concentrations of CO_2 than the C_3 pathway. Thus the evolution of C_4 plants may have occurred in response to a decrease in atmospheric CO_2 suspected on other grounds (Cerling *et al.*, 1993).

9.5.5.1 Isotopes in archaeology

The differences in nitrogen and carbon isotopic composition of various foodstuffs and the preservation of these isotope ratios in bone collagen provides a means of determining what ancient peoples ate. In the first investigation of bone collagen from human remains, DeNiro and Epstein (1981) concluded that Indians of the Tehuacan Valley in Mexico probably depended heavily on maize (a C_4 plant) as early as 4000 BC, whereas archeological investigations had concluded maize did not become important in their diet until perhaps 1500 BC. In addition, there seemed to be a steady increase in the dependence on legumes (probably beans) from 6000 BC to 1000 AD and a more marked increase in legumes in the diet after 1000 AD.

Mashed grain and vegetable charred onto potsherds during cooking provides an additional record of the diets of ancient peoples. DeNiro and Hasdorf (1985) found that vegetable matter subjected to conditions similar to burial in soil underwent large shifts in $\delta^{15}N$ and $\delta^{13}C$, but that vegetable matter that was burned or charred did not. The carbonization (charring, burning) process itself produced only small (2 or 3‰) fractionations. Since these fractionations are smaller than the range of isotopic compositions in various plant groups, they are of little significance. Since potsherds are among the most common artefacts recovered in archeological sites, this provides a second valuable means of reconstructing the diets of ancient peoples.

Figure 9.21 summarizes the results obtained in a number of studies of bone collagen and potsherds (DeNiro, 1987). Studies of several modern populations, including Eskimos and the Tlinglit Indians of the Northwestern US, were made as a control. Judging from the isotope data, the diet of Neolithic Europeans consisted entirely of C_3 plants and herbivores feeding on C_3 plants, in contrast to the Tehuacan Indians, who depended mainly on C_4 plants. Prehistoric peoples of the Bahamas and Denmark depended both on fish and on agriculture. In the case of Mesolithic Denmark, other evidence indicates the crops were C_3, and the isotope data bear this out. Although there is no corroborating evidence, the isotope data suggest the Bahamians also depended on C_3 rather than C_4 plants. The Bahamians had

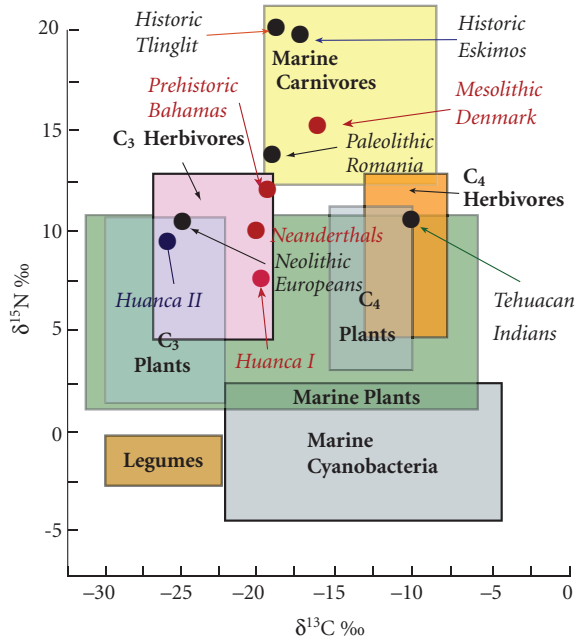

Figure 9.21 $\delta^{13}C$ and $\delta^{15}N$ of various foodstuffs and of diets reconstructed from bone collagen and vegetable matter charred onto pots by DeNiro and colleagues. The Huanca people were from the Upper Mantaro Valley of Peru. Data from potsherds of the Huanca I period (AD 1000–1200) suggest both C_3 and C_4 plants were cooked in pots, but only C_3 plants during the Huanca II period (AD 1200–1470). Adapted from DeNiro (1987). Reproduced with permission.

lower $\delta^{15}N$ because the marine component of their diet came mainly from coral reefs. Nitrogen fixation is particularly intense on coral reefs, which leads to ^{15}N depletion of the water, and consequently of reef organisms.

9.5.6 Isotopic "fossils" and the earliest life

As noted earlier, large carbon isotope fractionations are common to all autotrophs. Consequently, $\delta^{13}C$ values of –20‰ or less are generally interpreted as evidence of biologic origin of those compounds. Schidlowski (1988) first reported $\delta^{13}C$ as low as –26‰ in carbonate rocks from West Greenland that are ostensibly older than 3.5 Ga. Mojzsis *et al.* (1996) reported $\delta^{13}C$ between –20 to –50‰ for graphite inclusions in grains of apatite in 3.85 Ga banded-iron formations (BIFs) from the same area. In 1999, Rosing reported $\delta^{13}C$ of –19‰ from graphite in turbiditic and pelagic metasedimentary rocks from the Isua greenstone belt in the same area. These rocks are thought to be older than 3.7 Ga. In each case, these negative $\delta^{13}C$ values were interpreted as evidence of a biogenic origin of the carbon, and therefore that life existed on Earth at this time. This interpretation remains, however, controversial.

There are several reasons for the controversy, but all ultimately relate to the extremely complex geological history of the area. The geology of the region includes not only the early Archean rocks, but also rocks of middle and late Archean age as well. Most rocks are multiply and highly deformed and metamorphosed, and the exact nature, relationships, and structure of the precursor rocks are difficult to decipher. Indeed, Rosing (1999) argued that at least some of the carbonates sampled by Schidlowski (1988) are veins deposited by metamorphic fluid flow rather than metasediments. Others have argued that the graphite in these rocks formed by thermal decomposition of siderite ($FeCO_3$) and subsequent reduction of some of the carbon. Further effort will be needed to resolve this controversy.

9.6 PALEOCLIMATOLOGY

Perhaps one of the most successful and significant applications of stable isotope geothermometry has been paleoclimatology. At least since the work of Louis Agassiz* in 1840,

* Louis Agassiz (1807–1873) earned PhD and MD degrees from the Universities of Erlangen and Munich, respectively, in Germany before becoming professor of natural history at the University of Neuchâtel, specializing in ichthyology and paleontology. Based on the studies of glaciers and geomorphology in his native Switzerland, in 1840 Agassiz proposed that the Earth had experienced far colder temperatures, an *Ice Age*, in the recent past. In 1847, he became professor of zoology and natural history at Harvard University and also served as a visiting professor at Cornell University from its opening in 1865 until his death. By that time, Agassiz was perhaps the most famous scientist in the world.

geologists have contemplated the question of how the Earth's climate might have varied in the past. Until 1947, they had no means of quantifying paleotemperature changes. In that year, Harold Urey initiated the field of stable isotope geochemistry. In his classic 1947 paper, Urey calculated the temperature dependence of oxygen isotope fractionation between calcium carbonate and water and proposed that the isotopic composition of carbonates could be used as a paleothermometer. Urey's students and postdoctoral fellows empirically determined temperature dependence of the fractionation between calcite and water as:

$$T°C = 16.9 - 4.2\Delta_{\text{cal-H}_2\text{O}} + 0.13\Delta^2_{\text{cal-H}_2\text{O}} \quad (9.58)$$

For example, a change in $\Delta_{\text{cal-H}_2\text{O}}$ from 30 to 31 per mil implies a temperature change from 8° to 12°C. Urey suggested that the Earth's climate history could be recovered from oxygen isotope analyses of ancient marine carbonates. Although the problem has turned out to be much more complex than Urey anticipated, this has proved to be an extremely fruitful area of research. Deep-sea carbonate oozes contained an excellent climate record, and, as we shall see, several other paleoclimatic records are available as well.

9.6.1 The marine Quaternary $\delta^{18}O$ record and Milankovitch cycles

The principles involved in paleoclimatology are fairly simple. As Urey formulated it, the isotopic composition of calcite secreted by organisms should provide a record of paleoocean temperatures because the fractionation of oxygen isotopes between carbonate and water is temperature-dependent. In actual practice, the problem is somewhat more complex because the isotopic composition of the shell, or test, of an organism will depend not only upon temperature, but also upon the isotopic composition of the water in which the organism grew, "vital effects" (i.e., different species may fractionate oxygen isotopes somewhat differently), and post-burial isotopic exchange with sediment pore water. As it turns out, the vital effects and post-burial exchange are usually not very important for late Tertiary/Quaternary carbonates, but the isotopic composition of water is.

The first isotopic work on deep-sea sediment cores with the goal of reconstructing the temperature history of Pleistocene glaciations was by Cesare Emiliani (1955), who was then a student of Urey at the University of Chicago. Emiliani analyzed $\delta^{18}O$ in foraminifera from piston cores from the world's oceans. Remarkably, many of Emiliani's findings are still valid today, though they have been revised to various degrees. Rather than just the five glacial periods that geomorphologists had recognized, Emiliani found 15 glacial–interglacial cycles over the last 600,000 years. He found that these were global events, with notable cooling even in low latitudes, and concluded that the fundamental driving force for Quaternary climate cycles was variations in the Earth's orbit and consequent variations in the solar energy flux: *insolation*.

Emiliani had realized that the isotopic composition of the ocean would vary between glacial and interglacial times as isotopically light water was stored in glaciers, thus enriching the oceans in ^{18}O. He estimated that this factor accounted for about 20% of the observed variations. The remainder he attributed to the effect of temperature on isotope fractionation. Subsequently, Shackleton and Opdyke (1973) concluded that storage of isotopically light water in glacial ice was the main effect causing oxygen isotopic variations in biogenic carbonates, and that the temperature effect was only secondary.

The question of just how much of the variation in deep-sea carbonate sediments is due to ice build-up and how much is due to the effect of temperature on fractionation is an important one. The resolution depends, in part, on the isotopic composition of glacial ice and how much this might vary between glacial and interglacial times. It is fairly clear that the average $\delta^{18}O$ of glacial ice is probably less than –15‰, which Emiliani had assumed. Typical values for Greenland ice are –30 to –35‰ (relative to SMOW) and as low as –50‰ for Antarctic ice. If the exact isotopic composition of ice and the ice volume were known, it would be a straightforward exercise to calculate the effect of continental ice build-up on ocean isotopic composition. For example, the present volume of continental ice is $27.5 \times 10^6\,\text{km}^3$, while the volume of the oceans is $1350 \times 10^6\,\text{km}^3$. Assuming glacial ice has a mean $\delta^{18}O$ of –30‰ relative to

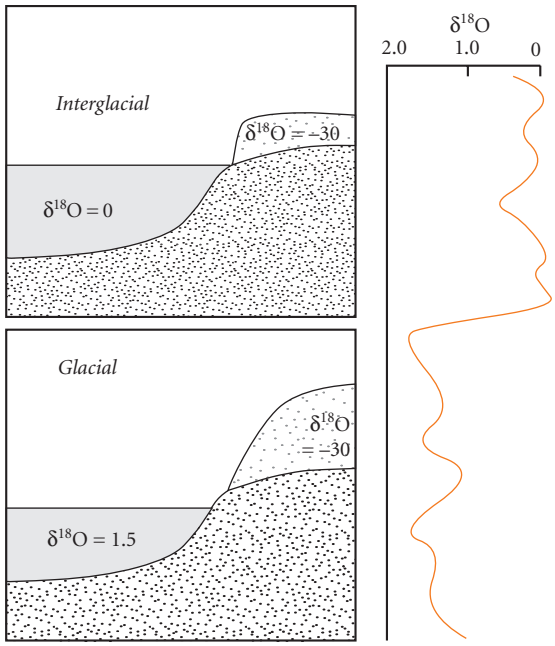

Figure 9.22 Cartoon illustrating how $\delta^{18}O$ of the ocean changes between glacial and interglacial periods.

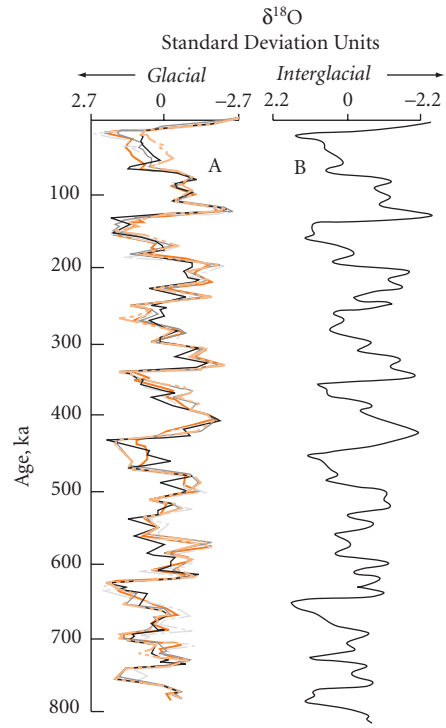

Figure 9.23 (A) "Stacking of five cores" selected by Imbrie *et al.* (1985). Because the absolute value of $\delta^{18}O$ varies from core to core, the variation is shown in standard deviation units. (B) Smoothed average of the five cores in A. From Imbrie (1985). Reproduced with permission.

SMOW, we can calculate the $\delta^{18}O$ of the total hydrosphere as –0.6‰ (neglecting freshwater reservoirs, which are small). At the height of the Wisconsinan Glaciation (the most recent one), the volume of glacial ice is thought to have increased by $42 \times 10^6 km^2$, corresponding to a lowering of sea level by 125 m. If the $\delta^{18}O$ of ice was the same then as now (–30‰), we can readily calculate that the $\delta^{18}O$ of the ocean would have increased by 1.59‰. This is illustrated in Figure 9.22.

We can use eqn. 9.58 to see how much the effect of ice volume on seawater $\delta^{18}O$ affects estimated temperature changes. According to this equation, at 20°C, the fractionation between water and calcite should be 33‰. Assuming present water temperature of 20°C, Emiliani would have calculated a temperature change of 6°C for an observed increase in the $\delta^{18}O$ of carbonates between glacial times and a present $\delta^{18}O$ of 2‰, after correction for 0.5‰ change in the isotopic composition of water. In other words, he would have concluded that surface ocean water in the same spot would have had a temperature of 14°C. If the change in the isotopic composition of water is actually 1.5‰, the calculated temperature difference is only about 2°C. Thus the question of the volume of glacial ice and its isotopic composition must be resolved before $\delta^{18}O$ in deep-sea carbonates can be used to calculate paleotemperatures.

Comparison of sea-level curves derived from dating of terraces and coral reefs indicate that each 0.011‰ variation in $\delta^{18}O$ represents a 1 m change in sea-level. Based on this and other observations, it is now generally assumed that the $\delta^{18}O$ of the ocean changed by about 1.5‰ between glacial and interglacial periods, but the exact value is still debated.

By now, thousands of deep-sea sediment cores have been analyzed for oxygen isotope ratios. Figure 9.23 shows the global $\delta^{18}O$ record constructed by averaging analyses from five key cores (Imbrie *et al.*, 1985). A careful examination of the global curve shows a periodicity of approximately 100,000 years. The same periodicity was apparent in Emil-

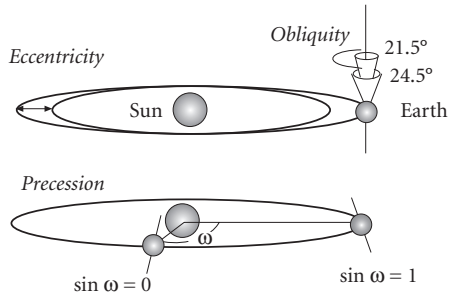

Figure 9.24 Illustration of the *Milankovitch parameters*. The eccentricity is the degree to which the Earth's orbit departs from circular. Obliquity is the tilt of the Earth's rotational axis with respect to the plane of the ecliptic and varies between 21.5° and 24.5°. Precession is the variation in the direction of tilt at the Earth's closest approach to the Sun (perihelion). The parameter ω is the angle between the Earth's position on June 21 (summer solstice), and perihelion.

iani's initial work and led him to conclude that the glacial–interglacial cycles were due to variations in the Earth's orbital parameters. These are often referred to as the Milankovitch cycles, after Milutin Milankovitch, a Serbian astronomer who argued in the 1920s and 1930s* that they caused the ice ages (Milankovitch, 1938).

Let's explore Milankovitch's idea in a bit more detail. The *eccentricity* (i.e., the degree to which the orbit differs from circular) of the Earth's orbit about the Sun and the degree of tilt, or *obliquity*, of the Earth's rotational axis vary slightly. In addition, the direction in which the Earth's rotational axis tilts varies, a phenomenon called *precession*. These variations are illustrated in Figure 9.24. Though variation in these "Milankovitch parameters" has negligible effect on the *total* radiation the Earth receives, they do affect the *pattern* of incoming radiation. For example, tilt of the rotational axis determines seasonality and the latitudinal gradient of insolation. The gradient is extremely important because it drives atmospheric and oceanic circulation. If the tilt is small, seasonality will be reduced (cooler summers, warmer winters). Precession relative to the eccentricity of the Earth's orbit also affects seasonality. For example, presently the Earth is closest to the Sun in January. As a result, northern hemisphere winters (and southern hemisphere summers) are somewhat warmer than they would be otherwise. For a given latitude and season, precession will result in a ±5% difference in insolation. While the Earth's orbit is only slightly elliptical, and variations in eccentricity are small, these variations are magnified because insolation varies with the inverse square of the Earth–Sun distance.

Variation in tilt approximates to a simple sinusoidal function with a period of 41,000 yrs. Variations in eccentricity can be approximately described with period of 100,000 years. In actuality, however, eccentricity variation is more complex, and is more accurately described with periods of 123,000 yrs, 85,000 yrs, and 58,000 yrs. Similarly, variation in precession has characteristic periods of 23,000 and 18,000 yrs.

Although Emiliani suggested that $\delta^{18}O$ variations were related to variations in these orbital parameters, the first quantitative approach to the problem was that of Hayes *et al.* (1976). They applied Fourier analysis to the $\delta^{18}O$ curve (Fourier analysis is a mathematical tool that transforms a complex variation such as that in Figure 9.23 to the sum of a series of simple sine functions). Hayes *et al.* then used spectral analysis to show that much of the spectral power of the $\delta^{18}O$ curve occurred at frequencies similar to those of the Milankovitch parameters. The most elegant and convincing treatment is that of Imbrie (1985). Imbrie's treatment involved several refinements and extension of the earlier work of Hayes *et al.* (1976). First, he used improved values for Milankovitch frequencies. Second, he noted that these Milankovitch parameters vary with time (the Earth's orbit and tilt are affected by the gravitational field of the Moon and other planets, and other astronomical events, such as bolide impacts), and the climate system's response to them might also

* While Milankovitch was a strong and early proponent of the idea that variations in the Earth's orbit caused ice ages, he was not the first to suggest it. J. Croll of the UK first suggested it in 1864, and published several subsequent papers on the subject.

vary over time. Thus Imbrie treated the first and second 400,000 years of Figure 9.23 separately.

Imbrie observed that climate does not respond instantaneously to forcing. For example, maximum temperatures are not reached in Ithaca, New York, until late July, 4 weeks after the maximum insolation, which occurs on June 21. Thus there is a *phase* lag between the forcing function (insolation) and climatic response (temperature). Imbrie (1985) constructed a model for response of global climate (as measured by the $\delta^{18}O$ curve) in which each of the six Milankovitch forcing functions was associated with a different gain and phase. The values of gain and phase for each parameter were found statistically by minimizing the residuals of the power spectrum of the $\delta^{18}O$ curve in Figure 9.23. The resulting "gain and phase model" is shown in comparison with the data for the past 400,000 years and the next 25,000 years in Figure 9.25. The model has a correlation coefficient, r, of 0.88 with the data. Thus about r^2, or 77%, of the variation in $\delta^{18}O$, and therefore presumably in ice volume, can be explained by Imbrie's Milankovitch model. The correlation for the period 400,000–782,000 yrs is somewhat poorer, around 0.80, but nevertheless impressive.

Since variations in the Earth's orbital parameters do not affect the average total annual insolation the Earth receives, but only its pattern in space and time, one might ask how this could cause glaciation. The key factor seems to be the insolation received during summer at high northern latitudes. This is, of course, the area where large continental ice sheets develop. The southern hemisphere, except for Antarctica, is largely ocean, and therefore not subject to glaciation. Glaciers apparently develop when summers are not warm enough to melt the winter's accumulation of snow in high northern latitudes.

Nevertheless, even at a given latitude the total variation in insolation is small, and not enough by itself to cause the climatic variations observed. Apparently, there are feedback mechanisms at work that serve to amplify the fundamental Milankovitch forcing function. One of these feedback mechanisms was identified by Agassiz, and that is ice albedo, or reflectance. Snow and ice reflect much of the incoming sunlight back into space. Thus

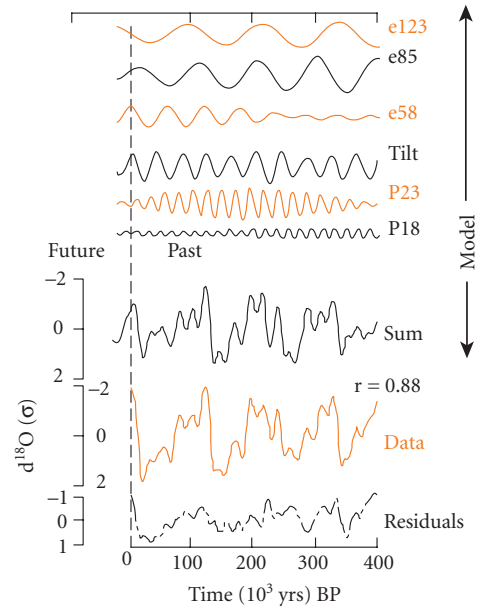

Figure 9.25 Gain and phase model of Imbrie, relating variations in eccentricity, tilt, and precession to the oxygen isotope curve. Top shows the variation in these parameters over the past 400,000 and next 25,000 years. Bottom shows the sum of these functions with appropriated gains and phases applied and compares them with the observed data. From Imbrie (1985). Reproduced with permission.

as glaciers advance, they will cause further cooling. Any additional accumulation of ice in Antarctica, however, does not result in increased albedo, because the continent is fully ice covered even in interglacial times – hence the dominant role of northern hemisphere insolation in driving climate cycles. Other possible feedback mechanisms include carbon dioxide and ocean circulation. The role of atmospheric CO_2 in controlling global climate is a particularly important issue because burning of fossil fuels has resulted in a significant increase in atmospheric CO_2 concentration over the last 150 years. We will return to this topic at the end of Chapter 12.

9.6.2 The record in glacial ice

Climatologists recognized early on that continental ice preserves a stratigraphic record of climate change. Some of the first ice cores recovered for the purpose of examining the climatic record and analyzed for stable iso-

topes were taken from Greenland in the 1960s (e.g., Camp Century Ice Core). Subsequent cores have been taken from Greenland, Antarctica, and various alpine glaciers. Very long ice cores that covered 150,000 years were recovered by the Russians from the Vostok station in Antarctica in the 1980s and were deepened over the next 20 years, eventually reaching back 400,000 years. In 2003, drilling began on the EPICA (European Project for Ice Coring in Antarctica) project Dome C Ice Core in Antarctica, which eventually drilled through 3260 m, corresponding to 800 ka of ice before halting just short of bedrock. Jouzel *et al.* (1987, 1993, 1996) focused on δD variations in these cores because it is more sensitive to temperature than is $\delta^{18}O$. In their initial work, temperatures were calculated from δD based on an empirical relationship between measured temperature and δD in Antarctic snow and after subtracting the effect of changing ice volume on δD of the oceans. In the most recent work, they used global circulation models to obtain the relationship between δD and temperature (Jouzel *et al.*, 2007). These recent results showed temperature variations of 15°C between glacial and interglacial times, and these variations track the marine isotope record well, as can be seen in Figure 9.26, except in the lowermost 60 m or so of ice, which showed evidence of being deformed.

Figure 9.27 compares temperatures calculated from the EPICA Antarctic core (lower line) with $\delta^{18}O$ in ice from the Greenland Ice Core Project (GRIP) (upper line). The Greenland ice record agrees well with the Antarctic one, although the former is limited to the last 120 ka, largely because ice accumulates much faster in Greenland. The high ice accumulation rates in Greenland limit the range of time covered by the record, but do provide high resolution. They reveal sharp changes in temperature and ice volume on time-scales of a millennium and less. These rapid fluctuations in climate are known as Dansgaard-Oeschager events and can be correlated to $\delta^{18}O$ variations in high-resolution sediment cores from the North Atlantic. The warming events correlate with temperature maxima in Antarctica, suggesting coupling of climate between the two hemispheres. The cause of these Dansgaard-Oeschager events is still unclear, but changes in the North Atlantic Ocean circulation, perhaps triggered by an influx of fresh water from melting glacier and icebergs, are suspected.

9.6.3 Soils and paleosols

As we found in Chapter 6, the concentration of CO_2 in soils is very much higher than in the atmosphere, reaching 1% by volume. As a result, soil water can become supersaturated with respect to carbonates. In soils where evaporation exceeds precipitation, soil carbonates form. The carbonates form in

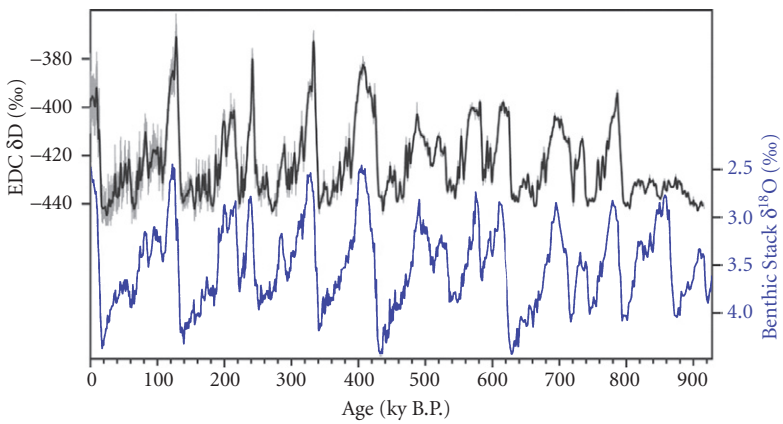

Figure 9.26 δD of ice in the EPICA Dome C ice core (upper line) compared with $\delta^{18}O$ of benthic foraminifera in deep-sea cores (lower line). Because the temperature variation in deep ocean water is small, the latter record mainly variations in ice volume. There is good overall agreement between the two cores. From Jouzel *et al.* (2007). Reprinted with permission from AAAS.

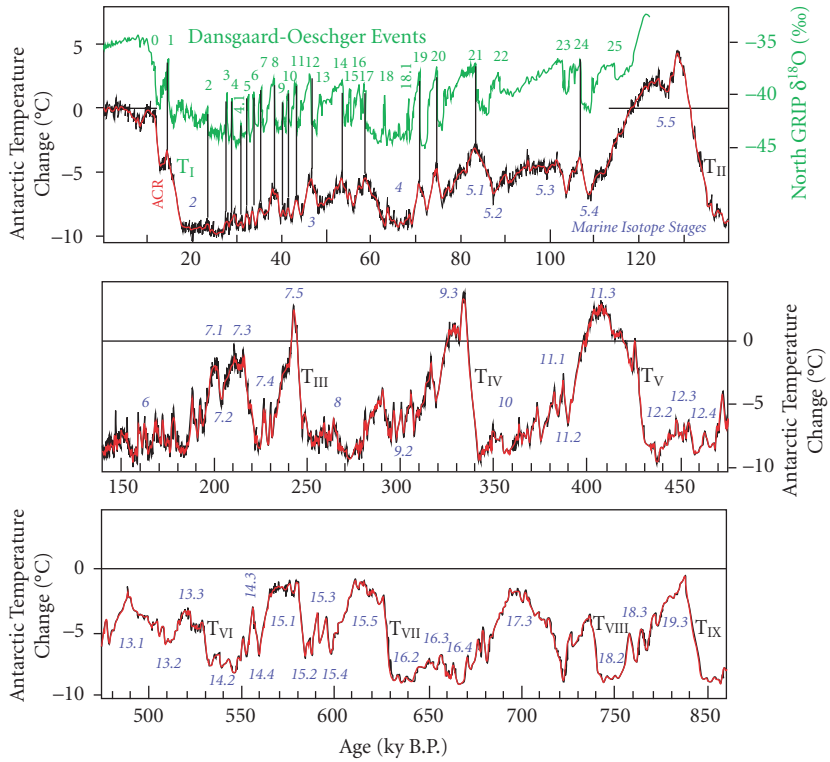

Figure 9.27 Antarctic temperature variation calculated from the EPICA ice core (lower line) compared with the $\delta^{18}O$ record from the GRIP ice core from Greenland (upper line). The former suggest a 15°C temperature range from the coldest glacial to the warmest interglacial period. From Jouzel *et al.* (2007). Reprinted with permission from AAAS.

equilibrium with soil water, and there is a strong correlation between $\delta^{18}O$ in soil carbonate and local meteoric water, though soil carbonates tend to be about 5‰ more enriched than expected from the calcite–water fractionation. There are two reasons why soil carbonates are heavier. First, soil water is enriched in ^{18}O relative to meteoric water due to preferential evaporation of isotopically light water molecules. Second, rain (or snow) falling in wetter, cooler seasons is more likely to run off than that falling during warm seasons. Taking these factors into consideration, the isotopic composition of soil carbonates may be used as a paleoclimatic indicator.

Figure 9.28 shows one example of $\delta^{18}O$ in paleosol carbonates used in this way. The same Pakistani paleosol samples analyzed by Quade *et al.* (1989) for $\delta^{13}C$ (Figure 9.20) were also analyzed for $\delta^{18}O$. The $\delta^{13}C$ values recorded a shift toward more positive values

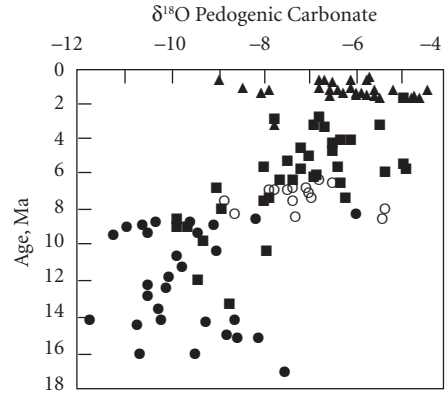

Figure 9.28 $\delta^{18}O$ in paleosol carbonate nodules from the Potwar Plateau in northern Pakistan. Different symbols correspond to different, overlapping sections that were sampled. Reprinted by permission from McMillan Publishers Ltd: Quade *et al.* (1989).

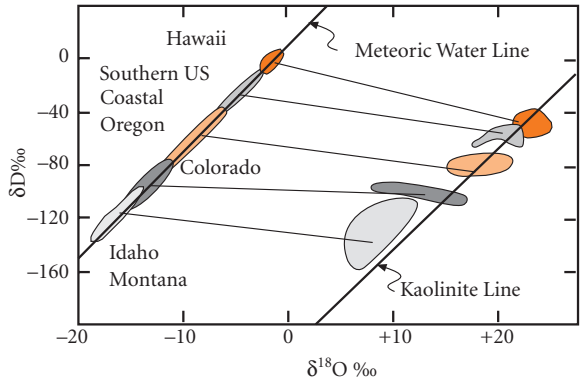

Figure 9.29 Relationship between δD and $\delta^{18}O$ in modern meteoric water and kaolinites. Kaolinites are enriched in ^{18}O by about 27‰ and ^{2}H by about 30‰. After Lawrence and Taylor (1972). With permission from Elsevier.

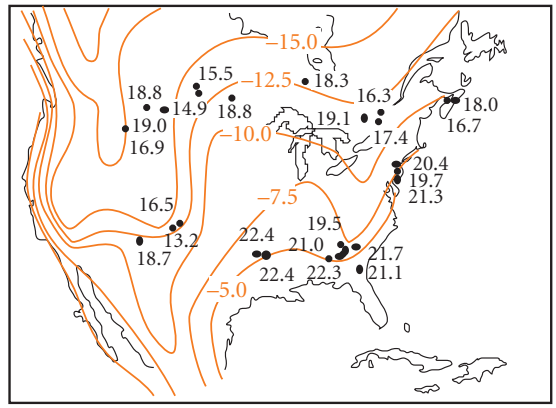

Figure 9.30 $\delta^{18}O$ in Cretaceous kaolinites from North American (in black) compared with contours of $\delta^{18}O$ (in red) of present-day meteoric water. After Lawrence and Meaux (1993).

at 7 Ma that apparently reflected the appearance of C_4 grasslands. The $\delta^{18}O$ shows a shift to more positive values at around 8 Ma, or a million years before the $\delta^{13}C$ shift. Quade *et al*. interpreted this as due to an intensification of the monsoon system at that time, an interpretation consistent with marine paleontological evidence.

Clays, such as kaolinites, are another important constituent of soil. Lawrence and Taylor (1972) showed that during soil formation, kaolinite and montmorillonite form in approximate equilibrium with meteoric water so that their $\delta^{18}O$ values are systematically shifted by +27‰ relative the local meteoric water, while δD values are shifted by about 30‰. Thus kaolinites and montmorillonites define a line parallel to the meteoric water line (Figure 9.29), the so-called *kaolinite line*. From this observation, Sheppard *et al*. (1969) and Lawrence and Taylor (1972) reasoned that one should be able to deduce the isotopic composition of rain at the time ancient kaolinites formed from their δD values. Since the isotopic composition of precipitation is climate-dependent, ancient kaolinites provide another continental paleoclimatic record.

There is some question as to the value of hydrogen isotopes in clays for paleoclimatic studies. Lawrence and Meaux (1993) concluded that most ancient kaolinites have exchanged hydrogen subsequent to their formation, and therefore are not good paleoclimatic indicators. Others argue that clays do not generally exchange hydrogen unless recrystallization occurs, or the clay experiences temperatures in excess of 60–80°C for extended periods (A. Gilg, personal communication, 1995).

Lawrence and Meaux (1993) concluded, however, that oxygen in kaolinite does preserve the original $\delta^{18}O$, and that it can, with some caution, be used as a paleoclimatic indicator. Figure 9.30 compares the $\delta^{18}O$ of ancient Cretaceous North American kaolinites with the isotopic composition of modern precipitation. If the Cretaceous climate were the same as the present one, the kaolinites should be systematically 27‰ heavier than modern precipitation. For the southeastern US, this is approximately true, but the difference is generally less than 27‰ for other kaolinites, and the difference decreases northward. This indicates that these kaolinites formed in a warmer environment than the present one. Overall, the picture provided by Cretaceous kaolinites confirms what has otherwise been deduced about Cretaceous climate: that it was generally warmer, and the equator to pole temperature gradient was lower. A drawback with this approach, however, is the lack of good ages on paleosols, which have proven to be very difficult to date precisely. The ages of many paleosols used by

Lawrence and Meaux (1993) were simply inferred from stratigraphy.

9.7 HYDROTHERMAL SYSTEMS AND ORE DEPOSITS

When large igneous bodies are intruded into high levels of the crust, they heat the surrounding rock and the water in the cracks and pores in this rock, setting up convection systems. The water in these hydrothermal systems reacts with the hot rock and undergoes isotopic exchange; the net result is that both the water and the rock change their isotopic compositions.

One of the first of many important contributions of stable isotope geochemistry to understanding hydrothermal systems was the demonstration by Harmon Craig (another student of Harold Urey) that water in these systems was meteoric, not magmatic (Craig, 1963). The argument is based upon the data shown in Figure 9.31. For each geothermal system, the δD of the "chloride" type geothermal waters is the same as the local precipitation and groundwater, but the $\delta^{18}O$ is shifted to higher values. The shift in $\delta^{18}O$ results from high-temperature reaction (≤300°C) of the local meteoric water with hot rock. However, because the rocks contain virtually no hydrogen, there is little change in the hydrogen isotopic composition of the water. If the water involved in these systems were magmatic, it would not have the same isotopic composition as local meteoric water (it is possible that these systems contain a few percent magmatic water).

Acidic, sulfur-rich waters from hydrothermal systems can have δD that is different from local meteoric water. This shift occurs when hydrogen isotopes are fractionated during boiling of geothermal waters. The steam produced is enriched in sulfide. The steam mixes with cooler meteoric water, condenses, and the sulfide is oxidized to sulfate, resulting in their acidic character. The mixing lines observed reflect mixing of the steam with meteoric water as well as fractionation during boiling.

Estimating temperatures at which ancient hydrothermal systems operated is a fairly straightforward application of isotope geothermometry, which we have already discussed. If we can measure the oxygen (or carbon or sulfur) isotopic composition of any two phases that were in equilibrium, and if

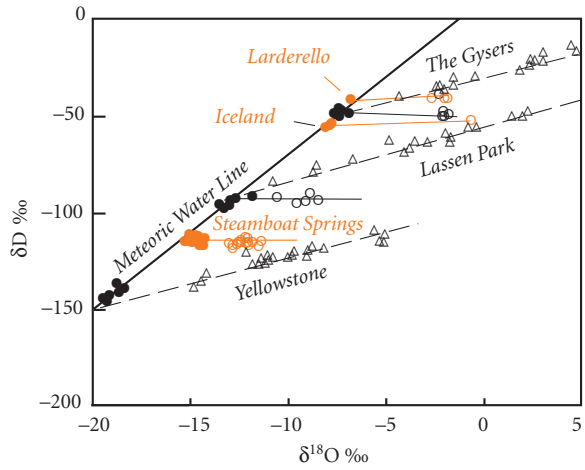

Figure 9.31 δD and $\delta^{18}O$ in meteoric hydrothermal systems. Closed circles show the composition of meteoric water in Yellowstone, Steamboat Springs, Mt. Lassen, Iceland, Larderello, and The Geysers, and open circles show the isotopic composition of chloride-type geothermal waters at those locations. Open triangles show the location of acidic, sulfide-rich geothermal waters at those locations. Solid lines connect the meteoric and chloride waters, dashed lines connect the meteoric and acidic waters. The "Meteoric Water Line" is the correlation between δD and $\delta^{18}O$ observed in precipitation in Figure 9.11. Source: From Craig, H. 1963. The isotopic composition of water and carbon in geothermal areas, in Nuclear Geology on Geothermal Areas, ed. by E. Tongiorgi, p. 17–53, Pisa: CNR Lab. Geol. Nucl. Reproduce with the permission of CNR Lab.

we know the fractionation factor as a function of temperature for those phases, we can estimate the temperature of equilibration. We will focus now on water–rock ratios, which may also be estimated using stable isotope ratios.

9.7.1 Water–rock ratios

For a closed hydrothermal system, we can write two fundamental equations. The first simply describes isotopic equilibrium between water and rock:

$$\Delta = \delta_w^f - \delta_r^f \qquad (9.59)$$

where we use the subscript w to indicate water, and r to indicate rock. The superscript

f indicates the final value. So eqn. 9.59 just says that the difference between the final isotopic composition of water and rock is equal to the fractionation factor (we implicitly assume equilibrium). The second equation is the mass balance for a closed system:

$$c_w W\delta_w^i + c_r R\delta_r^i = c_w W\delta_w^f + c_r R\delta_r^f \quad (9.60)$$

where *c* indicates concentration (we assume concentrations do not change, which is valid for oxygen, but perhaps not valid for other elements), *W* indicates the mass of water involved, *R* the mass of rock involved, the superscript *i* indicates the initial value and *f* again denotes the final isotope ratio. This equation just states the amount of an isotope present before reaction must be the same as after reaction. We can combine these equations to produce the following expression for the water–rock ratio:

$$\frac{W}{R} = \frac{\delta_r^f - \delta_r^i}{\delta_w^f - \delta_r^i}\frac{c_r}{c_w} \quad (9.61)$$

The initial $\delta^{18}O$ can generally be inferred from unaltered samples and from the δD–$\delta^{18}O$ meteoric water line, and the final isotopic composition of the rock can be measured. The fractionation factor can be estimated if we know the temperature and the phases in the rock. For oxygen, the ratio of concentration in the rock to water will be close to 0.5 in all cases.

Equation 9.61 is not very geologically realistic because it applies to a closed system. A completely open system, where water makes one pass through hot rock, would be more realistic. In this case, we might suppose that a small parcel of water, dW, passes through the system and induces an incremental change in the isotopic composition of the rock, $d\delta_r$. In this case, we can write:

$$Rc_r d\delta_r = \delta_w^i - [\Delta + \delta_r]c_w dW \quad (9.62)$$

This equation states that the mass of an isotope exchanged by the rock is equal to the mass of that isotope exchanged by the water (we have substituted $\Delta + \delta_r$ for δ_w^f). Rearranging and integrating, we have:

$$\frac{W}{R} = \ln\left(\frac{\delta_r^f - \delta_r^i}{-\delta_r^f + \delta_w^i - \Delta} + 1\right)\frac{c_w}{c_r} \quad (9.63)$$

Thus it is possible to deduce the water–rock ratio for an open system as well as a closed one.

Oxygen isotope studies can be a valuable tool in mineral exploration. Mineralization is often (though not exclusively) associated with the region of greatest water flux, such as areas of upward-moving hot water above intrusions. Such areas are likely to have the lowest values of $\delta^{18}O$. To understand this, let's solve eqn. 9.63 for δ_r^f, the final value of $\delta^{18}O$ in the rock:

$$\delta_r^f = \left(\delta_r^i - \delta_w^i + \Delta\right)e^{-\frac{Wc_w}{Rc_r}} + \delta_w^i + \Delta \quad (9.64)$$

Assuming a uniform initial isotopic composition of the rocks and the water, all the terms on the right-hand side are constants except *W/R* and Δ, which is a function of temperature. Thus the final values of $\delta^{18}O$ are functions of the temperature of equilibration, and an exponential function of the *W/R* ratio. Figure 9.32 shows $\delta^{18}O_r^f$ plotted as a function of *W/R* and Δ, where $\delta^{18}O_r^i$ is assumed to be +6 and $\delta^{18}O_w^i$ is assumed to be –13. In a few cases, ores apparently have precipitated from

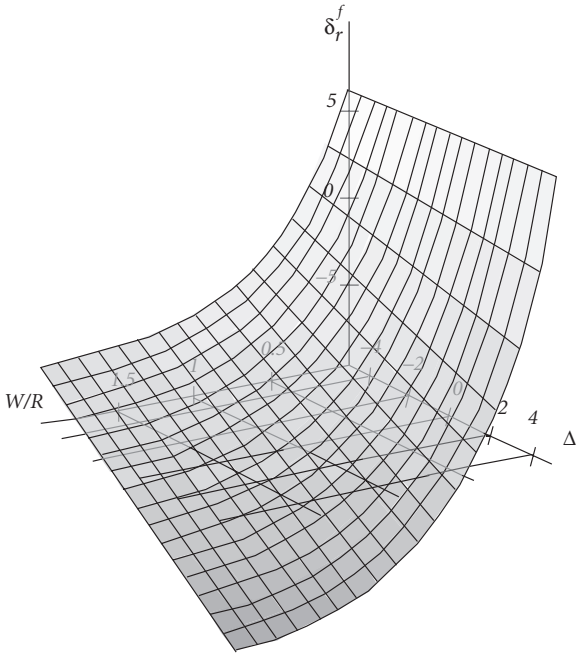

Figure 9.32 $\delta^{18}O$ as a function of *W/R* and Δ computed from eqn. 9.63.

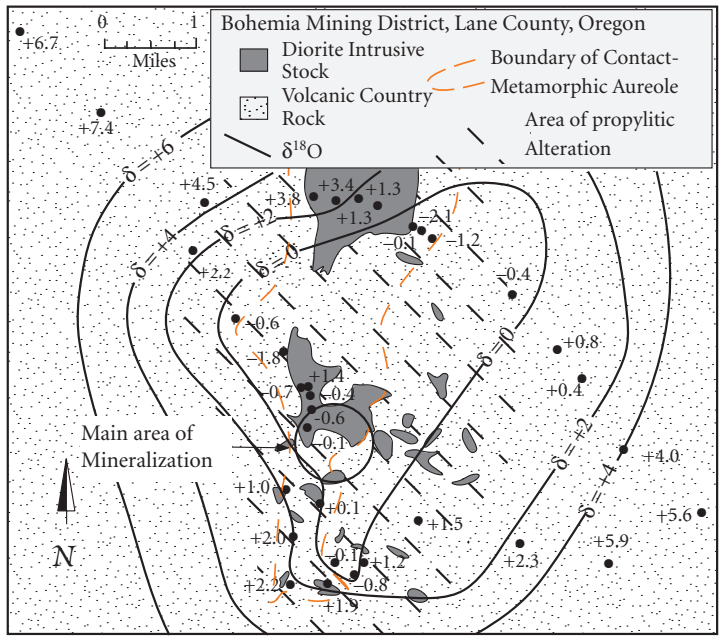

Figure 9.33 $\delta^{18}O$ variations in the Bohemia Mining District, Oregon. Note the bull's-eye pattern of the $\delta^{18}O$ contours. From Taylor (1974). Reproduced with permission.

fluids derived from the magma itself. In those cases, this kind of approach does not apply.

Figure 9.33 shows an example of the $\delta^{18}O$ imprint of an ancient hydrothermal system: the Bohemia Mining District in Lane County, Oregon, where Tertiary volcanic rocks of the western Cascades have been intruded by a series of dioritic plutons. Approximately $1,000,000 worth of gold was removed from the region between 1870 and 1940. $\delta^{18}O$ contours form a bull's-eye pattern, and the region of low $\delta^{18}O$ corresponds roughly with the area of propylitic (i.e., greenstone) alteration. Notice that this region is broader than the contact metamorphic aureole. The primary area of mineralization occurs within the $\delta^{18}O < 0$ contour. In this area, relatively large volumes of gold-bearing hydrothermal solution cooled, perhaps due to mixing with groundwater, and precipitated gold. This is an excellent example of the value of oxygen isotope studies to mineral exploration. Similar bull's-eye patterns are found around many other hydrothermal ore deposits.

9.7.2 Sulfur isotopes and ore deposits

A substantial fraction of base and noble metal ores are sulfides. These have formed in a great variety of environments and under a great variety of conditions. Sulfur isotope studies have been very valuable in sorting out the genesis of these deposits. Of the various stable isotope systems we will consider here, sulfur isotopes are undoubtedly the most complex. This complexity arises in part because there are five common valence states in which sulfur can occur in the Earth, +6 (e.g., $BaSO_4$), +4 (e.g., SO_2), 0 (e.g., S), −1 (e.g., FeS_2) and −2 (H_2S). Significant equilibrium fractionations occur between these valence states. Each of these valence states forms a variety of compounds, and fractionations can occur between these as well (e.g., Figure 9.8). Finally, sulfur is important in biological processes, and fractionations in biologically mediated oxidations and reductions are often different from fractionations in the abiological equivalents.

There are two major reservoirs of sulfur on the Earth that have uniform sulfur isotopic

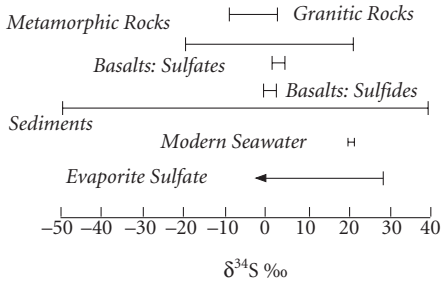

Figure 9.34 $\delta^{34}S_{CDT}$ in various geologic materials (adapted from Hoefs, 1987).

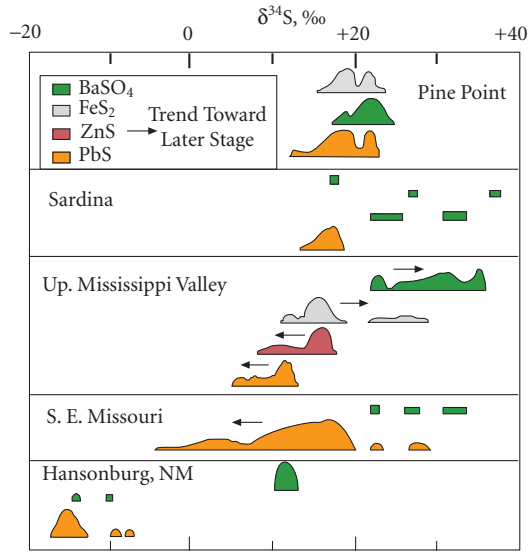

Figure 9.35 Sulfur isotope ratios in some Mississippi Valley-type Pb and Zn deposits. After Ohmoto and Rye (1979). With permission from John Wiley & Sons.

compositions: the mantle, which has $\delta^{34}S$ of ~0 and in which sulfur is primarily present in reduced form, and seawater, which has $\delta^{34}S$ of +20* and in which sulfur is present as SO_4^{2-}. Sulfur in sedimentary, metamorphic, and igneous rocks of the continental crust may have $\delta^{34}S$ that is either greater and smaller than these values (Figure 9.34). All of these can be sources of sulfide in ores, and further fractionation may occur during transport and deposition of sulfides. Thus the sulfur isotope geochemistry of sulfide ores is remarkably complex.

At magmatic temperatures, reactions generally occur rapidly and most systems appear to be close to equilibrium. Below 200°C, however, sulfur isotopic equilibration is slow even on geologic time-scales, hence equilibration is rare and kinetic effects often dominate. Isotopic equilibration between two sulfide species or between two sulfate species is achieved more readily than between sulfate and sulfide species. Sulfate–sulfide reaction rates have been shown to depend on pH (reaction is more rapid at low pH). In addition, equilibration is much more rapid when sulfur species of intermediate valences are present. Presumably this is because reaction rates between species of adjacent valance states (e.g., sulfate and sulfite) are rapid, but reaction rates between widely differing valence states (e.g., sulfate and sulfide) are much slower.

Mississippi Valley type deposits provide an interesting example of how sulfur isotopes can be used to understand ore genesis. These are carbonate-hosted lead and zinc sulfides formed under relatively low-temperature conditions. Figure 9.35 shows the sulfur isotope ratios of some examples. They can be subdivided into Zn-rich and Pb-rich classes. The Pb-rich and most of the Zn rich deposits were formed between 70–120°C, while some of the Zn-rich deposits, such as those of the Upper Mississippi Valley, were formed at temperatures up to 200°C, though most were formed in the range of 90–150°C.

Figure 9.36 illustrates a generalized model for the genesis of Mississippi Valley type deposits. In most instances, metals and sulfur appear to have been derived from distant sedimentary units, perhaps particularly from evaporites, by hot, deep-circulating formation water. In North America, most of these seem to have formed during or shortly after the late Paleozoic Appalachian-Ouchita-Marathon Orogeny. The direct cause of precipitation of the ore may have differed in the different localities. Oxygen and hydrogen isotope data suggest that mixing of the hot saline fluids

* This is the modern value for seawater. The sulfur isotopic composition of seawater is uniform at any time, but has varied over geologic time.

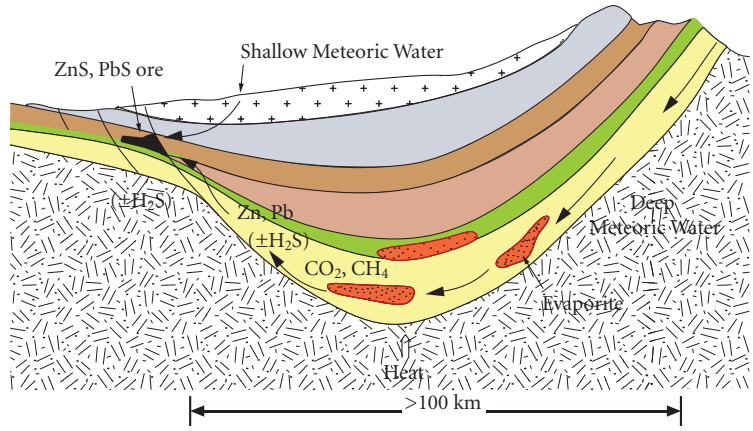

Figure 9.36 Cartoon illustrating the essential features of the genesis of Mississippi Valley sulfide ores. After Ohmoto (1986).

with cooler low-salinity ground water was probably the immediate cause of metal precipitation in some instances. In others, such as Pine Point, local reduction of sulfate to sulfide in the fluids may have caused precipitation (Ohmoto, 1986). Local production of sulfide shortly before ore deposition may help to account for the lack of isotopic equilibrium in this deposit, since time is an element in the attainment of isotopic equilibrium. In other cases, mixing of separate S-bearing and metal-bearing fluids from different aquifers may have been the cause.

The sulfur isotope data suggest there are a number of possible sources of sulfur. In many cases, sulfur was apparently derived from sulfate in evaporites; in others sulfur was derived from brines produced by evaporative concentration of seawater. In many cases, the sulfate was reduced by reaction with organic matter at elevated temperature (thermochemical reduction). In other cases, it may have been bacterially reduced. Other sulfur sources include sulfide from petroleum. In at least some deposits, sulfur appears to have been derived from more than one of these sources.

Sulfur isotope ratios in the SE Missouri district are quite variable and $\delta^{34}S$ is correlated with Pb isotope ratios in galenas. This suggests there was more than one source of the sulfur. Based on a combined Pb and S isotopic study, Goldhaber *et al.* (1995) concluded that the main-stage ores of the SE Missouri district were produced by mixing of fluids from several aquifers. They concluded that Pb was derived from the Lamont Sandstone (which directly overlies basement). Fluid in this aquifer was maintained at relatively high pε by the presence of hematite, and hence had low sulfide concentrations. This allowed leaching and transport of the Pb. Isotopically heavy S was produced by dissolution of evaporite sulfate and thermochemical reduction, and migrated through the Sillivan Siltstone member of the upper Bonneterre Formation, which overlies the Lamont Sandstone. Both Pb and isotopically light sulfur migrated through the lower part of the Bonneterre Formation. PbS precipitated when the fluids were forced to mix by pinchout of the Sillivan Siltstone.

9.7.3 Mass-independent sulfur isotope fractionation and the rise of atmospheric oxygen

In the modern Earth, variations in sulfur isotope ratios are almost always mass-dependent and $\delta^{33}S$ and $\delta^{36}S$ are related to variations in $\delta^{34}S$ as:

$$\delta^{33}S = 0.515 \times \delta^{34}S \quad \text{and} \quad \delta^{36}S = 1.90 \times \delta^{34}S$$

However, Farquhar *et al.* (2000) found that these relationships do not hold for sulfur in

many Archean sediments and ore deposits. Let's define the quantities $\Delta^{33}S$ and $\Delta^{36}S$ as:

$$\Delta^{33}S = \delta^{33}S - 0.515 \times \delta^{34}S \qquad (9.65)$$

and

$$\Delta^{36}S = \delta^{36}S - 1.90 \times \delta^{34}S \qquad (9.66)$$

Farquhar *et al.* found that many sulfides (primarily pyrite) in sediments and metasediments formed prior to 2500 Ma have positive $\Delta^{33}S$ and negative $\Delta^{36}S$, while hydrothermal sulfide ores and sedimentary sulfates (mainly barite) have negative $\Delta^{33}S$ and positive $\Delta^{36}S$ (Figure 9.37). During the Archean, $\Delta^{33}S$ (i.e., deviations from mass-dependent fractionation) of over 3‰ occurred. Farquhar *et al.* found smaller deviations, up to 0.5‰ in rocks from the period 2500–2000 Ma. They found no significant deviations from mass dependent fractionation in rocks younger than 2000 Ma.

This raises the obvious question of what process or processes operated during the Archean that could produce mass-independent fractionation? Why does this process no longer operate? As mentioned earlier, mass-independent isotope fractionation has been observed during laboratory photolysis of SO_2 and SO using ultraviolet light. This, together with the observation that ozone and molecular oxygen absorb ultraviolet radiation, provides a possible explanation. Modern volcanic eruptions loft vast quantities of SO_2 into the atmosphere, and Archean eruptions likely did so as well. If the Archean atmosphere lacked O_2 and O_3, ultraviolet radiation could penetrate deeply into it and photodissociate SO_2. According to experiments, these reactions produce sulfate with negative $\Delta^{33}S$ and elemental sulfur with positive $\Delta^{33}S$. The sulfate would dissolve in rain and ultimately find its way into the oceans. Some of this would precipitate as barite, $BaSO_4$. Some sulfate would be reduced in hydrothermal systems and precipitate as metal sulfides. Both these processes occur in modern oceans. The S would form particulate S_8 and also be swept out of the atmosphere by rain and ultimately incorporated into sediments, where it would react to form sedimentary sulfides. The latter also requires an absence of O_2 in the atmosphere – elemental S in the modern atmosphere would be quickly oxidized.

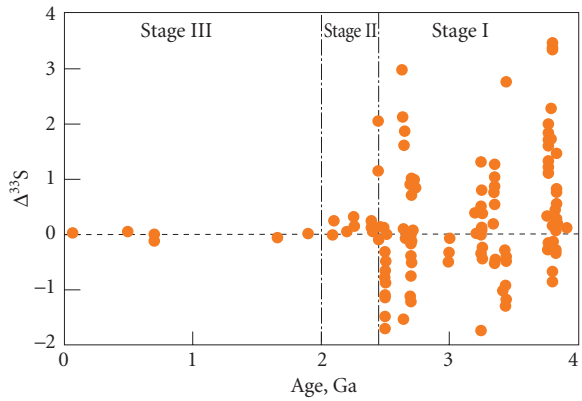

Figure 9.37 $\Delta^{33}S$ in sulfur through time. During Stage 1 (prior to 2.45 Ga), extensive mass-independent fractionation occurred as evidenced by $\Delta^{33}S$ up to 3.5‰, indicating the lack of atmospheric oxygen. During Stage 2 (2.45 to 2.0 Ga), limited amounts of atmospheric oxygen (up to 1% of present levels) absorbed most UV radiation and limited mass-independent fractionation to <0.5‰. High levels of atmospheric oxygen in Stage 3 (since 2.0 Ga) effectively eliminate UV radiation and mass-independent fractionation. Farquhar and Wing (2003). With permission from Elsevier.

Mass-independent fractionation in Archean sulfur thus provides evidence that the early atmosphere lacked free oxygen. This is entirely consistent with other evidence, such as the oxidation state of paleosols and detrital minerals, that the atmosphere did not contain significant amounts of O_2 until the early Proterozoic, about 2–2.3 billion years ago. Farquhar and Wing (2003) and Kasting and Catling (2003) provide excellent reviews on this topic.

9.8 STABLE ISOTOPES IN THE MANTLE AND MAGMATIC SYSTEMS

9.8.1 Stable isotopic composition of the mantle

The mantle is the largest reservoir for oxygen, and may be for H, C, N, and S as well. Thus we need to know the isotopic composition of the mantle to know the isotopic composition of the Earth. Variations in stable isotope ratios in mantle and mantle-derived materials also provide important insights on mantle and igneous processes.

9.8.1.1 Oxygen

Assessing the oxygen isotopic composition of the mantle, and particularly the degree to which its oxygen isotope composition might vary, has proved to be more difficult than expected. One approach has been to use basalts as samples of mantle, as is done for radiogenic isotopes. Isotope fractionation occurring during partial melting is small, so the oxygen isotopic composition of basalt should be similar to that of its mantle source. However, assimilation of crustal rocks by magmas and oxygen isotope exchange during weathering complicate the situation. An alternative is to use direct mantle samples such as xenoliths occasionally found in basalts. However, these are considerably rarer than are basalts.

Figure 9.38 shows the oxygen isotope compositions of olivines and clinopyroxenes in 76 peridotite xenoliths analyzed by Mattey *et al.* (1994) using the laser fluorination technique. The total range of values observed is only about twice that expected from analytical error alone, suggesting the mantle is fairly homogenous in its isotopic composition. The difference between coexisting olivines and clinopyroxenes averages about 0.5 per mil, which is consistent with the expected fractionation between these minerals at mantle temperatures. Mattey *et al.* (1994) estimated the bulk composition of these samples to be about +5.5 per mil.

Figure 9.39 shows the distribution of $\delta^{18}O$ in basalts from four different groups. To avoid weathering problems, Harmon and Hoefs (1995) included only submarine basaltic glasses and basalts having less than 0.75% water or have erupted historically in their compilation. There are several points worth noting in these data.

MORB has a mean $\delta^{18}O_{SMOW}$ of +5.7‰, with a relatively smaller variation about this mean. Thus the depleted upper mantle appears to be a relatively homogenous reservoir for oxygen. The homogeneity observed in MORB is consistent with that observed in mantle-derived xenoliths. The small difference between the means of the two groups (0.2‰), may well reflect fractionation occurring during partial melting.

The other groups show significantly greater heterogeneity than either MORB or peridotite

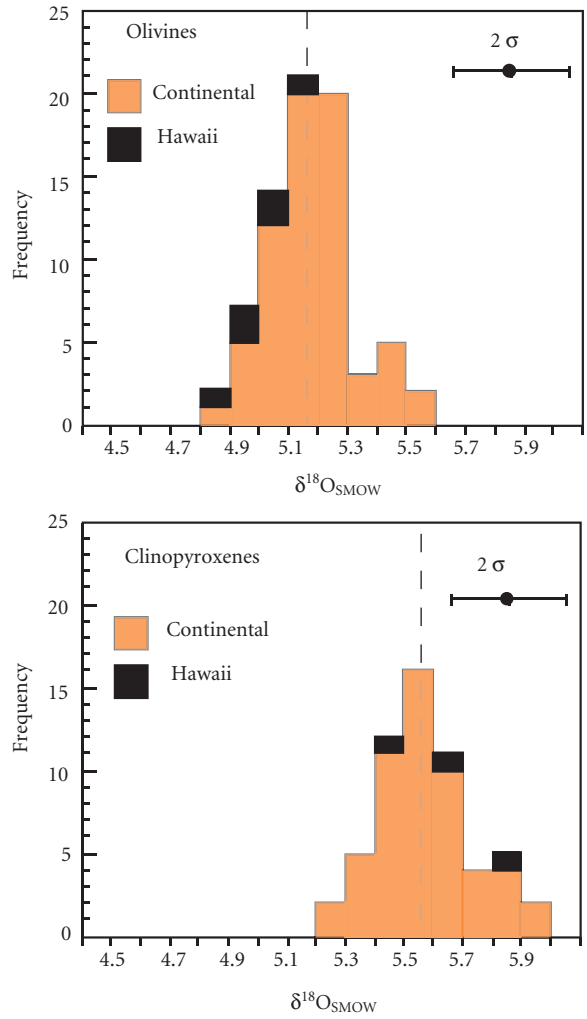

Figure 9.38 Oxygen isotope ratios in olivines and clinopyroxenes from mantle peridotite xenoliths. Data from Mattey *et al.* (1994). Reproduced by permission of the author.

xenoliths. Oceanic island basalts, which presumably sample mantle plumes, have a mean identical to that of peridotite xenoliths, but are more variable. Subduction-related basalts (i.e., island arc basalts and their continental equivalents) are shifted to more positive $\delta^{18}O$ values, as are continental intraplate volcanics.

Whether the variability in these groups reflects mantle heterogeneity, the melting process, assimilation, or merely weathering remains unclear. Hawaii is the one locality where high-quality data exists for both basalts and xenoliths and comparisons can be made. Both Hawaiian basalts and olivines in Hawai-